Low-x physics at LHC

Ronan McNulty[†]
School of Physics, University College Dublin, Dublin 4, Ireland.

Abstract
Collisions at the LHC sample a broad range of values in the $x - Q^2$ plane. Each of the LHC experiments have different acceptances and instrumentation that give them sensitivity to low-x physics through various experimental measurements: the cross-section for W and Z boson production; low mass Drell-Yan production; exclusive particle production in the forward region; and forward jet production. Measurements of these quantities will test the Standard Model, and constrain the parton distribution functions. Measurements of x as low as 10^{-6} appear possible that would allow tests of QCD in which saturation effects may be observed.

1 Introduction

Proton proton collisions at the LHC are fundamentally collisions between the constituent partons whose distribution, f, can be described as functions of x, the fractional momentum carried by the parton, and Q^2, the energy scale of the partonic collision. The cross-section, σ, for a process $pp \to X$ is a summation over all kinematically possible partonic processes $ab \to X$:

$$\sigma_X(Q^2) = \sum_{a,b} \int_0^1 dx_1 dx_2 f_a(x_1, Q^2) f_b(x_2, Q^2) \hat{\sigma}_{ab\to X}(x_1, x_2, Q^2) \tag{1}$$

The kinematic region accessible by the LHC operating at an energy of 14 TeV is shown by the largest shaded region in Figure 1. Experimentally, it is often easier to deal with rapidity, $y = \frac{1}{2}\ln(\frac{E+p_z}{E-p_z})$ of a particle with energy E or pseudo-rapidity, $\eta = \frac{1}{2}\ln(\frac{p+p_z}{p-p_z}) = -\ln\tan(\theta/2)$ where the z axis is coincident with the beam and $p_z = p\cos\theta$. The coverage of the four LHC experiments is compared in section 2: ATLAS and CMS are fully instrumented in the central rapidity region, $|\eta| < 2.5$ with some detectors in the forward region; LHCb is fully instrumented in the forward region, $1.9 < \eta < 4.9$; while ALICE has forward muon coverage and full tracking and calorimetry in the most central region $|\eta| < 0.9$.

In order to produce an object of mass Q at a rapidity of y, one requires partons with $x_1 = Qe^y/\sqrt{s}$ and $x_2 = Qe^{-y}/\sqrt{s}$. A rapidity axis is superimposed on the $x - Q^2$ axes in Figure 1 which, at least for light particles where $y \approx \eta$, allows the sensitivity of the LHC detectors to low-x physics to be judged. The central detectors can only access the low-x region by observing the production of low-Q^2 objects, while LHCb can access equivalent x-regions at higher Q^2. The dark shading in Figure 1 shows the regions where previous experiments have made measurements. The central LHC detectors, for the most part, overlap with previous experiments and in

[†]The author wishes to acknowledge the support of Science Foundation Ireland through grant 07-RFP-PHYF393

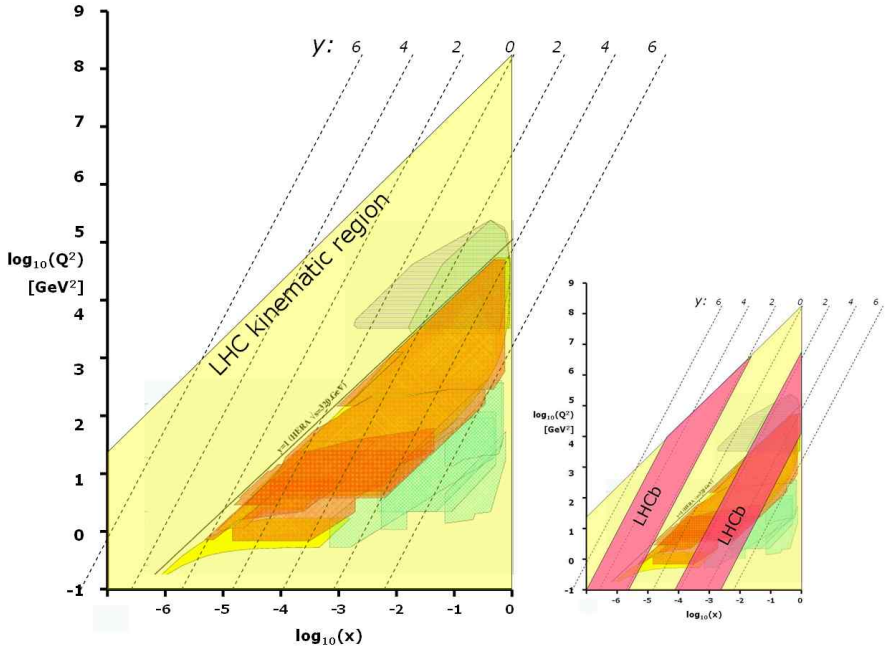

Fig. 1: Main figure: The region in $x - Q^2$ that is kinematically accessible to the LHC. Regions surveyed by previous experiments are indicated by darker shading. The insert shows the region that the LHCb experiment samples.

particular HERA, while LHCb samples one parton at high-x where many previous measurements exist, and one at very low-x where either no current data exists or DGLAP evolution [1] from lower Q^2 measurements at HERA is required.

Consequently the low-x region can be probed by the central detectors through low mass Drell-Yan production and the production of low mass resonances while LHCb and the forward components of ATLAS, CMS and ALICE can also look at forward resonances, forward jets, and higher mass Drell-Yan processes including W and Z production. These physics channels are examined below after making a brief survey of the different LHC detectors.

2 The LHC detectors

Figure 2 attempts to summarise, schematically, the coverage of the sub-detectors classified by function, of each of the LHC experiments. A brief description follows which includes an overview of the relevant triggers required to access the physics channels above.

The ATLAS [2] detector has tracking chambers inside $|\eta| < 2.5$, electromagnetic and hadronic calorimeters in $|\eta| < 4.9$, and muon chambers in $|\eta| < 2.7$. In addition they have counters (LUCID), primarily for luminosity measurements, in $5.6 < |\eta| < 6.0$, and counters and hadronic calorimeters (ZDC) in the far forward regions $|\eta| > 8.3$ They can trigger on muons and electrons with transverse momenta down to 4 GeV/c.

The CMS [3] detector's primary tracking also covers $|\eta| < 2.5$, however TOTEM [4]

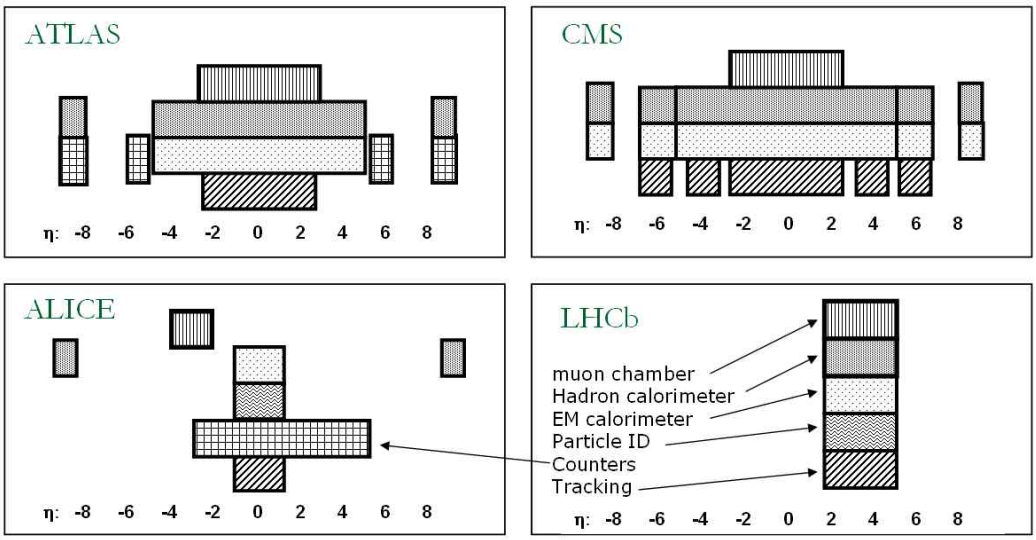

Fig. 2: A schematic representation of each of the LHC detectors where the horizontal axis is pseudorapidity. The functionality of the subdetectors is indicated by the shading as labelled.

extends the coverage into the forward region with tracking stations at $3.1 < |\eta| < 4.7$ and $5.2 < |\eta| < 6.5$. Electromagnetic and hadronic calorimetry are present in $|\eta| < 6.5$ Muon chambers are present in the central region: $|\eta| < 2.5$. They can trigger on muons and electrons down to transverse momenta of 3.5 GeV/c.

ALICE [5] has tracking, electromagnetic and handronic calorimeters inside $|\eta| < 0.9$. However, muon chambers occupy the region $-4 < \eta < -2.5$ and counters exist in the extended region $-3.4 < \eta < 5$. They can trigger on muons down to transverse momenta of 1 GeV/c.

LHCb [6] is fully instrumented with tracking, calorimetry, muon chambers and particle identification through RICH detectors, between $1.8 < \eta < 4.9$. They can trigger on muons down to transverse momenta of 1 GeV/c and hadrons of 2.5 GeV/c.

3 Forward W and Z production

The production of vector bosons is not what one would first consider to be low-x physics, and indeed in the central region the x of both partons are roughly similar, $x_1 \approx x_2 \approx 0.005$ and the scattering occurs between sea quarks. However, in the forward region in which LHCb is sensitive, x_1 lies between 0.04 and 0.8 while x_2 is between 4×10^{-5} and 8×10^{-4} and the scattering is more likely to occur between valence and sea quarks. The partonic cross-section for W and Z production is known to about 1%, so most of the uncertainty in the cross-section calculation resides in the knowledge of the PDFs at low x values. PDFs in the region $Q^2 \approx 10^4$ GeV^2, $4 \times 10^{-5} < x < 8 \times 10^{-4}$ have never been directly measured before so a measurement of W and Z production is also a test of the DGLAP evolution from experiments at lower Q^2.

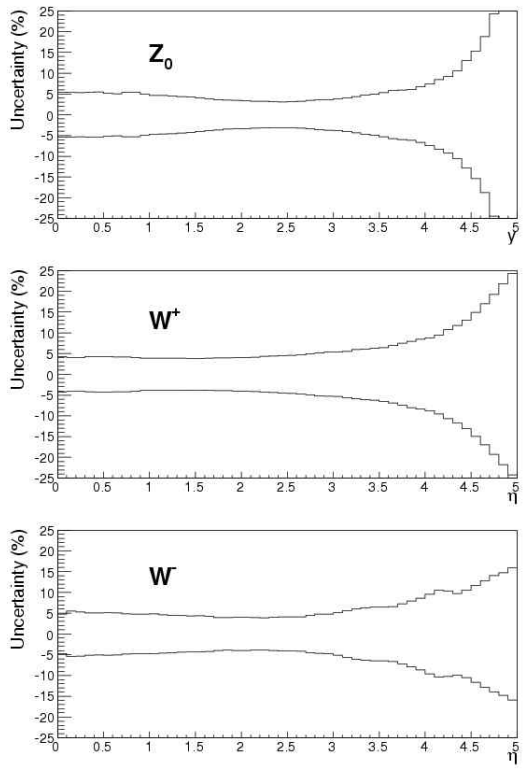

Fig. 3: The 90% confidence level band on the Z cross-section as a function of rapidity and W+,W- cross-sections as a function of the daughter lepton pseudorapidity. The cross-sections were calculated using the MCFM generator with the NNPDF parton distribution set.

The effect of current knowledge of the parton distribution functions (PDFs) on the vector boson cross-section predictions is shown in Fig 3 which was produced using the MCFM generator [7] with the NNPDF [8] parton distribution functions and shows the percentage uncertainties on the vector boson distributions as a function of Z boson rapidity, and the pseudorapidity of the lepton coming from the W.

LHCb have studied the sensitivity of their detector to this physics [9]. Z bosons can be reconstructed in the channel $Z \rightarrow \mu\mu$. The efficiency for triggering and reconstructing two high transverse momentum muons is high: $> 90\%$. The Z can easily be isolated from competing backgrounds, predominantly semileptonic B decays, by requiring high muon transverse momentum, isolation of each muon, and compatibility with the primary vertex. Less than 0.5% background remains in a window of 20 GeV/c^2 around the Z mass. The high efficiency and large cross-section mean that a statistical precision of 2.5% will be obtained with just 10 pb^{-1} of data, falling to below 1% after 100 pb^{-1}. Thus the measurement quickly becomes dominated by systematic uncertainties. It seems likely that detector effects influencing the efficiency estimate can be controlled to better than 0.5% leaving the dominant uncertainty to be the estimation of the machine luminosity which may reach a precision of 1 to 2% using channels such as the elastic production of exclusive dimuon events. [10, 11]

W bosons can be identified by LHCb in the channel $W \rightarrow \mu\nu$ and can be triggered with high efficiency, ($> 90\%$), by the requirement of a single high transverse momentum muon. Background processes are reduced by requiring that apart from the muon, there is little other activity in the event. The largest backgrounds come from Z events where only one muon enters the LHCb acceptance, and from high momentum pions or kaons which are misidentified as muons either because they decay in flight or they punch-through to the muon chambers. With suitable cuts on the muon momentum and the rest of the activity in the event, a signal efficiency of about 35% can be obtained with a purity of 85%. A statistical uncertainty better than 1% can thus be obtained after 10 pb^{-1} of data. Apart from the luminosity determination, the largest systematic is likely to

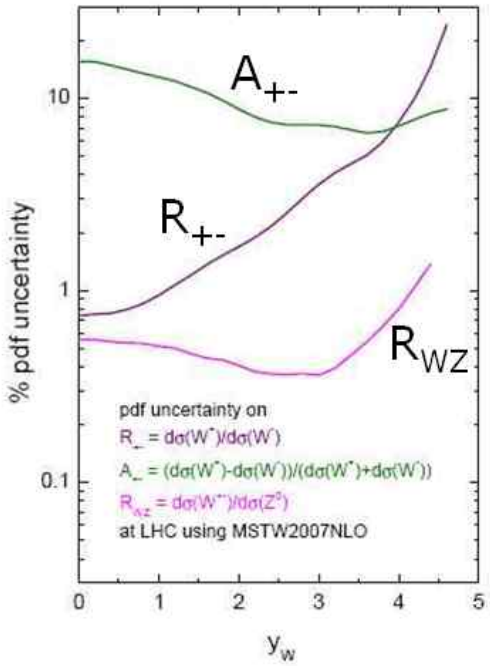

Fig. 4: The percentage uncertainty at the 90% confidence limit on R_{WZ}, R_{+-} and A_{+-} calculated using the MSTW2007NLO PDF set.

be due to the estimation of the background; however one is not overly reliant on the simulation in calculating this since background test samples can be produced from the data itself. It is expected that a systematic uncertainty below 1% can be attributed leaving the dominant systematic uncertainty, as for the Z analysis, coming from the luminosity determination.

One way to remove the luminosity uncertainty is to look at ratios of cross-sections. Rather than comparing $\sigma_Z, \sigma_{W+}, \sigma_{W-}$ to theory, one can consider the combinations [12, 13]:

$$R_{WZ} = \frac{(\sigma_{W+} + \sigma_{W-})}{\sigma_Z}, \;\; R_{+-} = \frac{\sigma_{W+}}{\sigma_{W-}}, \;\; A_{+-} = \frac{(\sigma_{W+} - \sigma_{W-})}{(\sigma_{W+} + \sigma_{W-})}. \tag{2}$$

The experimental uncertainty on these quantities will be less than 1% while Figure 4 (from [13]) shows the theoretical uncertainty coming from knowledge of the PDFs, as a function of rapidity. R_{WZ} is insensitive to the PDFs and the most sensitive test of the Standard Model occurs between $2 < y < 3$. However R_{+-} in the LHCb range, is dominated by the uncertainty on the d-valence quark distribution, and A_{+-} is dominated by the uncertainty on the difference in the u-valence and d-valence distributions. An experimental measurement at the 1% level will thus signficantly improve our knowledge of the PDFs.

4 Central and Forward Drell-Yan production

The production of muon or electron pairs through the Drell-Yan production of a virtual photon allows one to access a lower range in x: Figure 1 shows that moving to lower Q^2 for a given rapidity, moves one to smaller x. Thus the x range accessible to LHCb at a Q corresponding to the Z mass is accessible to ATLAS and CMS when looking at a photon of about 5 GeV/c^2. The cross-section for such processes is very much larger than for the Z; however the backgrounds are even bigger meaning that the overall experimental uncertainties in this channel will be greater.

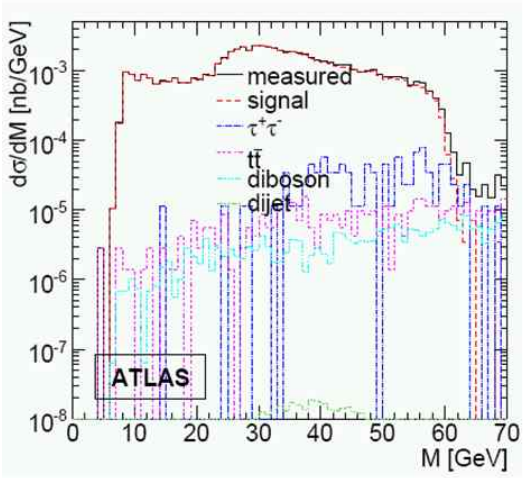

Fig. 5: Signal and estimated background for electron pairs produced by Drell-Yan interactions as a function of the invariant mass of the electrons, for the ATLAS experiment.

ATLAS have examined the production of electron pairs [14] and have sensitivity down to photon masses of 8 GeV/c^2, this limit being determined by the threshold on the transverse momentum of their electron trigger. They require two oppositely charged electrons in events where the missing transverse energy is less than 30 GeV. Figure 5 shows the signal well separated from the background coming from tau pairs, top events, W pairs, and dijets. This last background has the largest uncertainty due to finite Monte Carlo statistics. A statistical precision of 7% is expected in the mass range from 8 to 60 GeV/c^2 with 50 pb^{-1} of data.

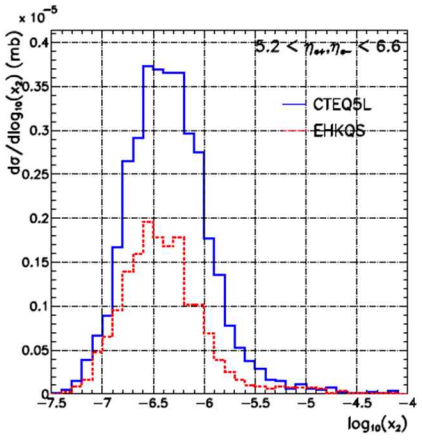

Fig. 6: Differential cross-section for electron pairs selected by CMS and TOTEM using two PDF sets, with and without saturation effects.

CMS have examined the same channel [15] but in the very forward region using the TOTEM detector. They trigger on events that deposit more than 300 GeV in the electromagnetic calorimeters and less than 5 GeV in the hadronic calorimters with one or more charged particles between $5.2 < |\eta| < 6.5$. Events with a di-electron invariant mass above 4 GeV/c^2 are selected. This signal probes values of x down to 10^{-6} and is potentially sensitive to saturation effects as can be seen in Figure 6 (from [15]) where the cross-section has been computed with one of the standard CTEQ [16] PDF sets, and with a particular saturation scheme as described by EHKQS [17]. The effect of background events is being evaluated.

LHCb [9] have performed a study in the channel with two muons in the final state. Very low trigger thresholds can be placed on muons in LHCb; the summed transverse momenta of both muons must only exceed 1.6 GeV/c and thus very low Q^2 are accessible.

The problem however lies in extracting a clean signal at such low invariant masses due to the overwhelming background coming from semi-leptonic b and c quark decays, as well as detector effects in mis-identifying pions and kaons as muons. A multi-variate selection has been employed in order to select events which have little missing energy and little other activity apart from the two muons.

Reasonably pure samples appear possible; $> 70\%$ for photon masses above 5 GeV/c^2 which would access x values of 2×10^{-6}. A full systematic study is ongoing and is likely to be limited by the precision with which the efficiency and purity of the selection can be determined, since the multi-variate selection is quite sensitive to the details of the simulation, and in particular, the underlying event.

However, a very precise experimental value is not required in order to improve the current theory, particularly in the forward region. Figure 7 (from [13]) shows the theoretical uncertainty on the Drell-Yan cross-section due to the PDFs as a function of rapidity, for two different masses. Even a total experimental uncertainty of 10% in measuring the cross-section for masses of 8 GeV/c^2 will improve the current theory. At lower masses and high rapidities, there is essentially no theoretical prediction because there is no HERA data at such low x values to evolve from.

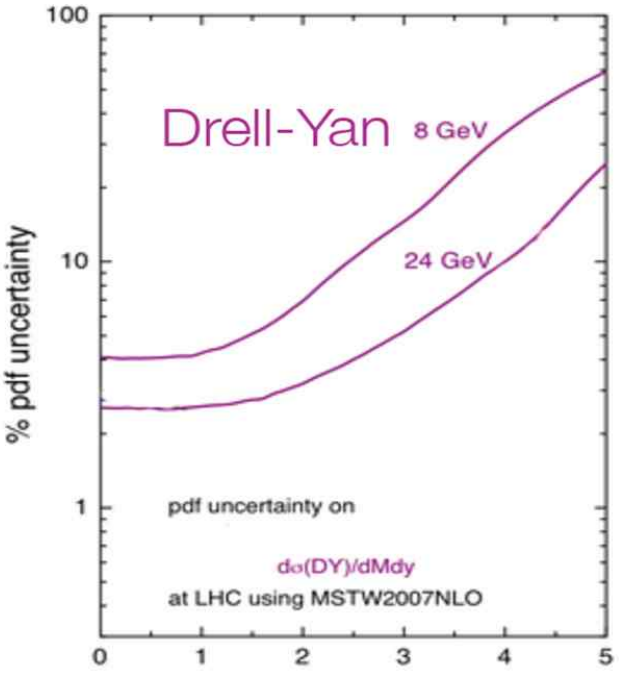

Fig. 7: The percentage uncertainty at the 90% confidence level on the cross-section as a function of rapidity for the Drell-Yan process at two mass scales, calculated using the MSTW2007NLO parton distribution set.

5 Exclusive Particle Production

The exclusive production of dimuons at the LHC is interesting both in terms of the physics that it accesses and the uses to which these channels can be put. CDF recently published results for this final state [18]. Two distinct processes are seen: firstly a continuum where the muons are produced through $\gamma\gamma$ interactions. and secondly the presence of resonances indicating charmonium production through photon-pomeron interactions.

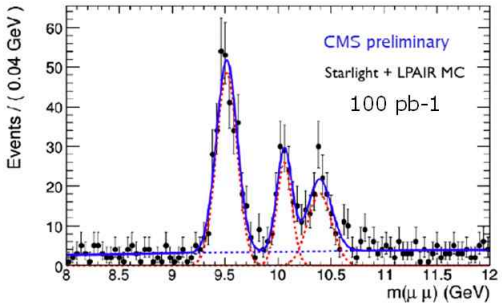

Fig. 8: Preliminary CMS result showing the expected resolution with which exclusive bottomonium production could be observed with 100pb^{-1} of data.

The former process is of particular interest in measuring the LHC luminosity since it is theoretically known to better than 1% and several studies have been performed by CMS, ATLAS and LHCb [10, 11]. The latter process is important in describing the pomeron and in searches for odderons. The low thresholds on the muon trigger at LHCb mean they will quickly be able to see the J/Ψ and Ψ' resonances that CDF have already observed, and in addition make observations of exclusive bottomonium production. ALICE, making use of their forward muon detectors, should be able to observe J/Ψ [19] which will probe x regions down to 10^{-6}. CMS have made a preliminary study of bottomonium production [11], and some results are shown in Figure 8 which indicates that clear $\Upsilon, \Upsilon', \Upsilon''$ signals will be visible with 100pb^{-1} of data.

6 Forward jet production

Accessing the low-x region through jet production requires excellent calorimetry in the forward region. CMS have investigated the number of events they would be able to see with a transverse energy threshold of 10 GeV using their calorimeters in the range $3 < |\eta| < 5$. Figure 9 from [11] shows the largest number of events occurs at the energy threshold and for $x_1 \approx 10^{-1}, x_2 \approx 10^{-4}$. Such events have the potential to probe x down to 10^{-5}. A full systematic study is underway as confronting data with theory will require a good understanding of the effects of hadronisation and the underlying event on the definition of the jet energy.

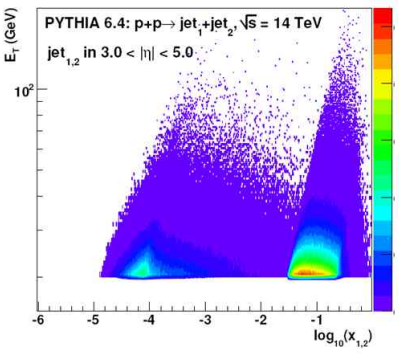

Fig. 9: The relationship between the E_T of a forward jet produced in CMS and the x values that are probed.

7 Conclusions

The four LHC experiments are instrumented to cover a wide range of the kinematically available $x - Q^2$ plane. Low-x physics is possible at central rapidities through low-Q^2 Drell-Yan production and in the forward region through Drell-Yan production of photons, W and Z, as well as through the production of jets and exclusive final states. These measurements will test the Standard Model and constrain the PDFs which is essential for the understanding of many putative New Physics signals. They will also allow further investigations of QCD and may be in a position to observe the onset of saturation effects.

References

[1] V.N. Gribov, L.N. Lipatov, Sov. J.Nucl. Phys. 15 (1972) 438;
Yu.L. Dokshitzer, Sov. Phys. JETP 46 (1977) 641;
G. Altarelli, G. Parisi, Nucl. Phys. B126 (1977) 298.

[2] The ATLAS Collaboration, G. Aad et al., *The ATLAS Experiment at the CERN Large Hadron Collider*, JINST 3 (2008) S08003.

[3] The CMS Collaboration, S Chatrchyan et al., *The CMS experiment at the CERN LHC* (2008) JINST 3 S08004.

[4] The TOTEM Collaboration, G Anelli et al., *The TOTEM Experiment at the CERN Large Hadron Collider* (2008) JINST 3 S08007.

[5] The ALICE Collaboration, K Aamodt et al., *The ALICE experiment at the CERN LHC* (2008) JINST 3 S08002.

[6] The LHCb Collaboration, A Augusto Alves Jr et al., *The LHCb Detector at the LHC* (2008) JINST 3 S08005.

[7] M. Campbell, R.K. Ellis, Phys. Rev. D62:114012 (2000).

[8] NNPDF Collaboration, R.D.Ball et al., *A Determination of parton distributions with faithful uncertainty estimation* (2009) Nucl.Phys.B809:1-63.

[9] R.McNulty, *Potential PDF sensitivity at LHCb*, Proc. DIS2008, London, doi:10.3360/dis.2008.29

[10] A.G. Shamov, V.I. Telnov, Nucl. Inst. Meth. **A494** (2002) 51.
B. Caron, *Luminosity Measurement at the Large Hadron Collider*, Thesis: University of Alberta 2006, CERN-THESIS-2006-024.
J.S. Anderson, *Testing the electroweak sector and determining the absolute luminosity at LHCb using dimuon final state*, Ph.D. Thesis: University College Dublin. 2008.

[11] S. Ovyn, *Exclusive dilepton and Upsilon production with CMS: A feasibility study.* Proc. DIS2008, London, CERN-CMS-CR-2008-036, doi:10.3360/dis.2008.78

[12] A.D. Martin et al., *Parton Distributions and the LHC: W and Z Production*, hep-ph/9907231.

[13] R. Thorne et al., *Parton Distributions and QCD at LHCb* Proc. DIS2008, London, arXiv:0808.1847, doi:10.3360/dis.2008.30

[14] J. Katzy *First physics prospects with the ATLAS detector at LHC.* ATL-COM-2008-064

[15] CMS and TOTEM collaborations, *Prospect for diffractive and forward physics at LHC*, CERN/LHCC 2006-039/G-124.

[16] H.L. Lai et al. *Global QCD analysis of parton structure of the nucleon: CTEQ5 parton distributions* Eur.Phys.J.C12:375-392,2000.

[17] K.J. Eskola et al.,*Nonlinear corrections to the DGLAP equations in view of the HERA data*, Nucl. Phys. B 660 (2003) 211.

[18] T. Aaltonen et al., *Observation of Exclusive Charmonium Production and* $\gamma\gamma \to \mu^+\mu^-$ *in* $p\bar{p}$ *Collisions at* $\sqrt{s} = 1.96$ *TeV* arXiv:0902.1271.

[19] T. Shears, *Access to small x Parton Density Functions at the LHC* Proc. ISMD 2008, DESY, Hamburg, DESY-PROC-2009-001. arXiv:0902.0377.